J|A|C|S
ARTICLES
Published on Web 03/26/2005

Spin-Crossover Dendrimers: Generation Number-Dependent Cooperativity for Thermal Spin Transition

Tsuyohiko Fujigaya,[†] Dong-Lin Jiang,*[,§] and Takuzo Aida*[,†,§]

Contribution from the Department of Chemistry and Biotechnology, School of Engineering, The University of Tokyo, 7-3-1 Hongo, Bunkyo-ku, Tokyo 113-8656, Japan, and Aida Nanospace Project, Exploratory Research for Advanced Technology (ERATO), Japan Science and Technology Agency (JST), 2-41 Aomi, Koto-ku, Tokyo 135-0064, Japan

Received January 15, 2005; E-mail: jiang@nanospace.miraikan.jst.go.jp (D.-L.J.); aida@macro.t.u-tokyo.ac.jp (T.A.)

Abstract: Poly(benzyl ether) dendrons having a focal triazole unit (G*n*trz: trz = triazole; *n* = generation number = 0−2) were found to react with $(MeSO_3)_2Fe$ to form dendritic coordination polymers ($[Fe(Gntrz)_3](MeSO_3)_2 \cdot 2H_2O$) that undergo the thermal spin transition. When the generation number of the dendritic unit was larger ($n = 0 \rightarrow 1 \rightarrow 2$), the average degree of polymerization ($D_p = 20 \rightarrow 10 \rightarrow 3$) and spin-crossover temperature ($T_c = 335 \rightarrow 315 \rightarrow 300$ K) of the resulting polymer were lower. However, the abruptness of the spin transition was not monotonically dependent on the generation number; (G1trz)Fe exhibited an abrupt spin transition with a temperature width of only 10 K, while the smallest and largest members of the (G*n*trz)Fe family both displayed a rather broad spin-transition temperature width (30 (n = 0) and 50 K (n = 2)). X-ray diffraction and calorimetric analyses indicated the presence of a discotic columnar core−shell assembly with a crystal lattice best occupied by a C_{3v} symmetric array of medium-sized (G1trz)-Fe.

Introduction

Self-assembly of dendritic macromolecules is an interesting subject from a fundamental viewpoint[1] and has also been studied in relation to the self-organization events in biological systems. To develop novel functional soft materials with a nanometric structural precision, recent studies have focused on self-assembly of molecularly engineered dendritic macromolecules to form large hierarchical structures with enhanced complexities.[2] Selected examples include formation of donor−acceptor CT complexes in low-dimensional columnar and nanotubular assemblies,[3] combination of condensation and cross-linking chemistries to form hollow architectures,[4] construction of a hydrogen-bonded network within a crystalline paraffinic domain to form self-assembled proton channels,[5] and interconnection of dendrimers into an ordered template−dendrisilica nanocomposite.[6] Along the line of these studies, one may expect that dendritic macromolecules when precisely organized should generate a long-range cooperation phenomenon that may account for the enhancement of certain functions. However, this interesting possibility has not yet been well explored to date. In the present paper, we investigated spin-crossover properties of self-assembled poly(benzyl ether) dendrimers bearing an iron(II) triazolate focal core (Scheme 1). Triazole derivatives are known to coordinate with iron(II) to form self-assembled coordination polymers, where the iron(II) centers can adopt two different spin states, that is, low-spin and high-spin states that are interconvertible upon external stimuli (spin crossover).[7] The spin transition from low-spin to high-spin is accompanied by a slight elongation of the metal−ligand bonds, leading to a volume expansion of the coordination sphere around the metal center. Among several parameters to evaluate spin-crossover properties, abruptness of thermal spin transition is informative of how the self-assembled components are cooperative with one another.[8]

[†] The University of Tokyo.
[§] JST.

(1) (a) Fréchet, J. M. J.; Tomalia, D. A. *Dendrimers and Other Dendritic Polymers*, VCH−Wiley: New York, 2000. (b) Narayanan, V. N.; Newkome, G. R. *Top. Curr. Chem.* **1998**, *197*, 19−77. (c) Bosman, A. W.; Janssen, H. M.; Meijer, E. W. *Chem. Rev.* **1999**, *99*, 1665−1688. (d) Tomalia, D. A. *Aldrichimica Acta* **2004**, *37*, 39−57.
(2) (a) Serrette, A. G.; Swager, T. M. *J. Am. Chem. Soc.* **1993**, *115*, 8879−8880. (b) Lehmann, M.; Sierra, T.; Barber, J.; Serrano, J. L.; Parker, R. *J. Mater. Chem.* **2002**, *12*, 1342−1350. (c) Percec, V.; Johansson, G.; Heck, J.; Ungar, G.; Batty, S. V. *J. Chem. Soc., Perkin Trans. 1* **1993**, 1411−1420. (d) Percec, V.; Johansson, G.; Ungar, G.; Zhou, J. *J. Am. Chem. Soc.* **1996**, *118*, 9855−9866. (e) Percec, V.; Cho, W.-D.; Ungar, G.; Yeardley, D. J. P. *Chem.−Eur. J.* **2002**, *8*, 2011−2025. (f) Percec, V.; Holerca, M. N.; Uchida, S.; Cho, W.-D.; Ungar, G.; Lee, Y.; Yeardley, D. J. P. *Chem.−Eur. J.* **2002**, *8*, 1106−1117.
(3) (a) Percec, V.; Glodde, M.; Bera, T. K.; Miura, Y.; Shiyanovskaya, I.; Singer, K. D.; Balagurusamy, V. S. K.; Heiney, P. A.; Schnell, I.; Rapp, A.; Spiess, H.-W.; Hudson, S. D.; Duan, H. *Nature* **2002**, *417*, 384−387. (b) Yamaguchi, T.; Ishii, N.; Tashiro, K.; Aida, T. *J. Am. Chem. Soc.* **2003**, *125*, 13934−13935.
(4) (a) Schultz, L. G.; Zhao, Y.; Zimmerman, S. C. *Angew. Chem., Int. Ed.* **2001**, *40*, 1962−1966. (b) Kim, Y.; Mayer, M. F.; Zimmerman, S. C. *Angew. Chem., Int. Ed.* **2003**, *42*, 1121−1126.
(5) Percec, V.; Dulcey, A. E.; Balagurusamy, V. S. K.; Miura, Y.; Smidrkal, J.; Peterca, M.; Nummelin, S.; Edlund, U.; Hudson, S. D.; Heiney, P. A.; Duan, H.; Magonov, S. N.; Vinogradov, S. A. *Nature* **2004**, *430*, 764−768.
(6) Landskron, K.; Ozin, G. A. *Science* **2004**, *306*, 1529−1532.
(7) (a) Kahn, O.; Launay, J. P. *Chemtronics* **1988**, *3*, 140−151. (b) Kahn, O.; Kröber, J.; Jay, C. *Adv. Mater.* **1992**, *4*, 718−728. (c) Real, J. A.; Gaspar, A. B.; Niel, V.; Munoz, M. C. *Coord. Chem. Rev.* **2002**, *236*, 121−141. (d) Roubeau, O.; Haasnoot, J. G.; Codjovi, E.; Varret, F.; Reedijk, J. *Chem. Mater.* **2002**, *14*, 2559−2566. (e) Koningsbruggen, P. J.; Garcia, Y.; Codjovi, E.; Lapouyade, R.; Kahn, O.; Fournes, L.; Rabardel, L. *J. Mater. Chem.* **1997**, *7*, 2069−2075. (f) Garcia, Y.; Koningsbruggen, P. J.; Codjovi, E.; Lapouyade, R.; Khan, O.; Rabardel, L. *J. Mater. Chem.* **1997**, *7*, 857−858.

10.1021/ja050275k CCC: $30.25

Scheme 1. Synthesis of (G*n*trz)Fe ($n = 0-2$)

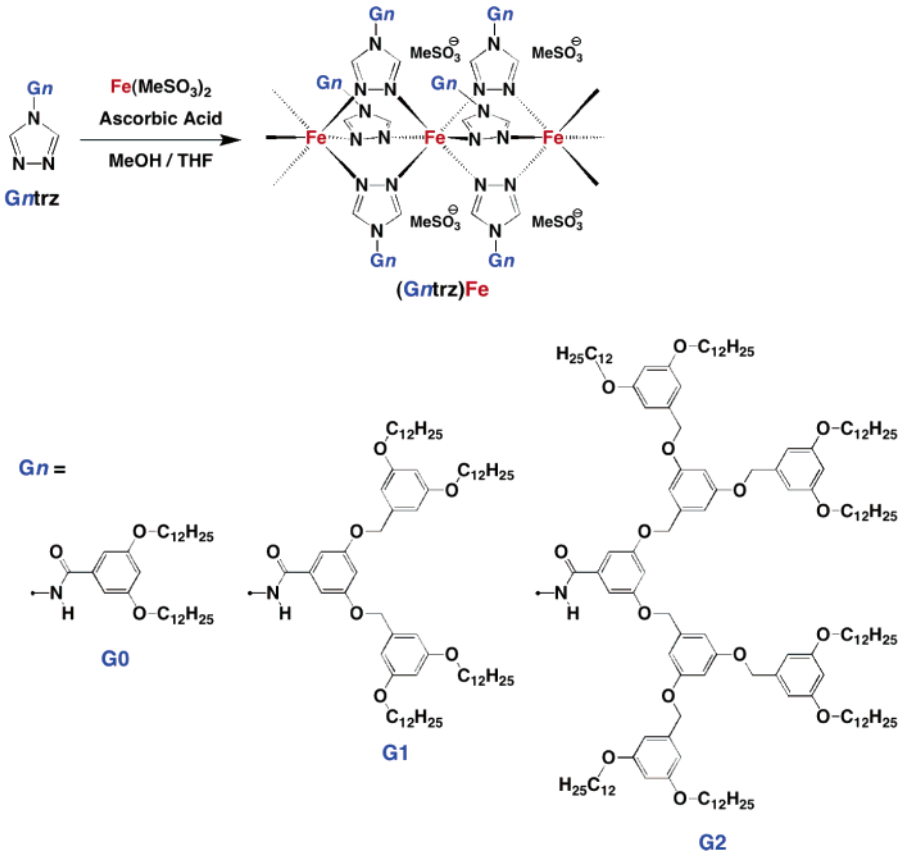

According to theoretical predictions,[9] long-range cooperativity is also an important factor for the realization of photoinduced spin crossover. In the present paper, we report the thermal spin-transition properties of iron(II) complexes of dendritic triazoles with different generation numbers (G*n*trz)Fe ($n = 0-2$), along with their self-assembled structures and calorimetric properties, and highlight a clear generation number dependency of the abruptness of the thermal spin transition.

Results and Discussion

Synthesis of Dendritic Triazole Ligands G*n*trz ($n = 0-2$) and their Iron(II) Complexes (G*n*trz)Fe ($n = 0-2$). In a manner similar to that reported previously,[10] alkyl-tethered poly(benzyl ether) dendritic triazoles with different generation numbers (Scheme 1; G*n*trz, $n = 0-2$) were newly synthesized by a DBOP-mediated coupling of 4-amino-1,2,4-triazole with poly(benzyl ether) dendrons bearing a carboxylic acid focal core (DBOP = diphenyl(2,3-dihydro-2-thioxo-3-benzoxazolyl)phosphonate)[11] and unambiguously characterized by means of MALDI-TOF-MS spectrometry, together with ^{1}H and ^{13}C NMR, and IR spectroscopies. G*n*trz ($n = 0-2$), thus obtained, were allowed to react with $Fe(MeSO_3)_2 \cdot 3 \cdot 1H_2O$ in THF/MeOH (1/5 vol), and their iron(II) complexes, (G*n*trz)Fe (Scheme 1; $n = 0-2$), were isolated as insoluble precipitates. Figure 1 shows infrared (IR) spectra of G*n*trz and (G*n*trz)Fe ($n = 0-2$). By reference to G*n*trz ($n = 0-2$), (G0trz)Fe−(G2trz)Fe all displayed a red shift of the N═C−N vibrational band (1550 cm^{-1}) due to the coordination with iron(II),[12] along with four new vibrational bands assignable to O═S═O (bending, $\delta_{sym} = 554$ and $\delta_{asym} = 776$ cm^{-1}; stretching, $\nu_{sym} = 1046$ and $\nu_{asym} = 1206$ cm^{-1}) in the counteranion (SO_3^-). EXAFS of (G0trz)Fe displayed at 23 °C short-range peaks at 1.9, 2.7, 3.6, and 3.9 assignable to Fe^1-N,[4] Fe^1-N^3/C,[5] Fe^1-Fe^2, and Fe^1-N^1/C^2, respectively, and also a long-range $Fe^1-Fe^2-Fe^3$ scattering at 7.3 Å (Figure 2A).[13] One-generation higher (G1trz)Fe showed a similar spectral feature to that of (G0trz)Fe (Figure 2B). However, the highest-generation (G2trz)Fe displayed only broad EXAFS peaks without any detectable long-range scattering at 7.3 Å (Figure 2C).

Magnetic Susceptibilities of (G*n*trz)Fe ($n = 0-2$). (G0trz)-Fe was colored violet at room temperature with a characteristic broad absorption band centered at 553 nm due to a $d-d$ electronic transition of the low-spin iron(II) species (Figure 3, red curve). Upon heating, decoloration took place to give off-white solid materials, as a result of the thermally induced spin transition to the high-spin state (Figure 3, blue curve). (G1trz)-Fe and (G2trz)Fe displayed a similar absorption spectral change on heating. As shown in Figure 4, (G0trz)Fe−(G2trz)Fe, upon

(8) Kahn, O.; Jay, C. *Science* **1998**, *279*, 44−48.
(9) Ogawa, Y.; Koshihara, S.; Takesada, M.; Ishikawa, T. *Mol. Cryst. Liq. Cryst.* **2002**, *379*, 357−364.
(10) Fujigaya, T.; Jiang, D.-L.; Aida, T. *J. Am. Chem. Soc.* **2003**, *125*, 14690−14691.
(11) Ueda, M.; Kameyama, A.; Hashimoto, K. *Macromolecules* **1988**, *21*, 19−24.
(12) Sinditskii, V. P.; Sokol, V. I.; Fogel'zang, A. E.; Dutov, M. D.; Serushkin, V. V.; Porai-Koshits, M. A.; Svtelov, B. S. *Russ. J. Inorg. Chem.* **1987**, *32*, 1149−1153.
(13) (a) Michalowicz, A.; Moscovic, J.; Garcia, Y.; Kahn, O. *J. Synchrotron Rad.* **1999**, *6*, 231−232. (b) Yokoyama, T.; Murakami, Y.; Kiguchi, M.; Komatsu, T.; Kojima, N. *Phys. Rev. B* **1998**, *58*, 14238−14244. (c) Garcia, Y.; Moscovic, J.; Michalowicz, A.; Ksenofontov, V.; Gevchenko, G.; Bravi, G.; Chasseau, D.; Gütlich, P. *Chem.—Eur. J.* **2002**, *8*, 4992−5000. (d) Michalowicz, A.; Moscovici, J.; Ducourant, B.; Cracco, D.; Kahn, O. *Chem. Mater.* **1995**, *7*, 1833−1842.

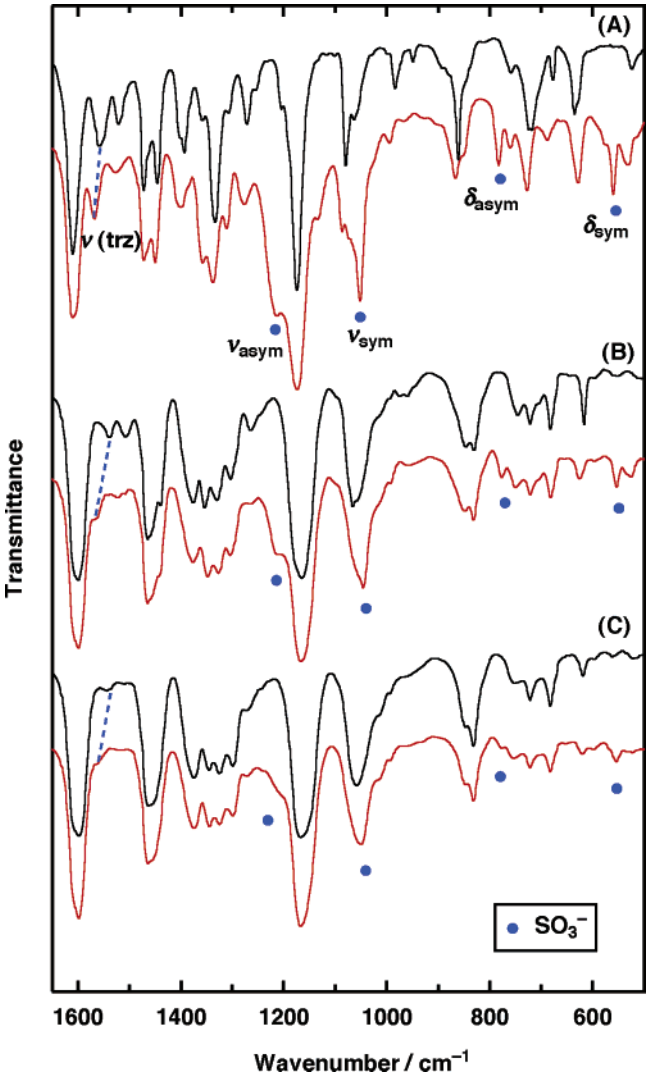

Figure 1. Infrared (IR) spectra of G*n*trz (black curves) and (G*n*trz)Fe (red curves); $n = 0$ (A), $n = 1$ (B), and $n = 2$ (C) at 23 °C.

heating from 240 to 350 K, showed a notable increase in molar magnetic susceptibility χT up to 3.5 cm^3 K mol^{-1}.[14] One may also note here that the spin-transition profile on heating is highly dependent on the generation number (n) of the dendritic unit. In general, temperature dependencies of χT are closely related to the coordination environments around the metal centers. From the spin-transition profiles on heating, it is obvious that the temperature range (ΔT) required for complete spin transition is only 10 K for (G1trz)Fe. Accordingly, the decoloration profile on heating also displayed an abrupt response to the temperature change (Figure 4B, inset). In sharp contrast, (G0trz)Fe and (G2trz)Fe on heating did not show such an abrupt spin-transition profile, and ΔT values of 30 and 50 K, respectively, were observed. We also noticed that the spin-crossover temperature, T_c (the temperature at which one-half of the spin transition is complete), is highly dependent on the generation number of the dendritic wedge; T_c decreased from 335 to 315 to 300 K as the generation number (n) increased from 0 to 1 to 2.

(14) As is known for some other iron(II) sulfonate complexes,[7d−f] the spin transition of (G*n*trz)Fe bearing a sulfonate anion was not thermoreversible because of the loss of water in the heating process. Water is known to play an essential role in the spin crossover of iron(II) sulfonate complexes. In fact, when colorless (G1trz)Fe, after the spin transition from low-spin to high-spin states, was kept under wet conditions below T_c, it gradually reverted to the purple-colored low-spin state. Although (G0trz)Fe behaved similarly, a longer immersion under wet conditions was necessary for the spin transition to the low-spin state.

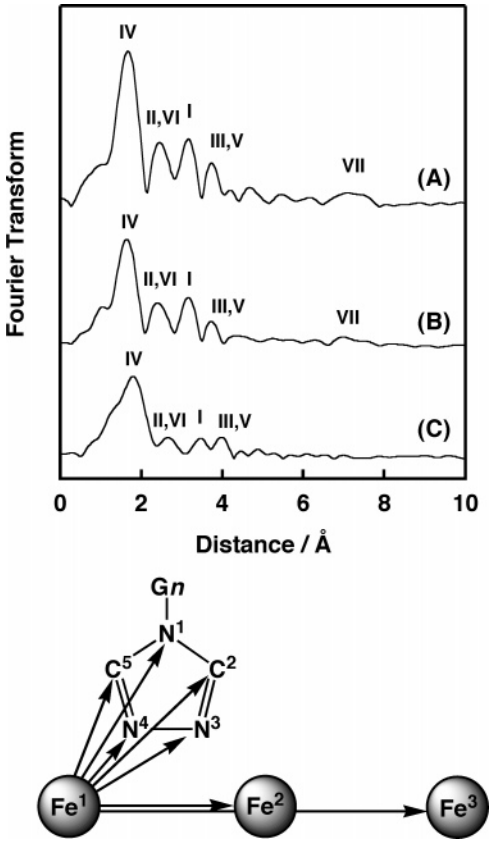

Figure 2. EXAFS spectra of (G0trz)Fe (A), (G1trz)Fe (B), and (G2trz)Fe (C). Assignments. IV: A scattering from Fe^1−N^4 in an octahedral coordination sphere of FeN$_6$. II and VI: Scatterings from Fe^1−C^5 (II) and Fe^1−N^3 (VI). I: A scattering from Fe^1−Fe^2. III and V: Scatterings from Fe^1−C^2 (III) and Fe^1−N^1 (V). VII: A multiple scattering from a linear Fe^1−Fe^2−Fe^3 polymeric structure.

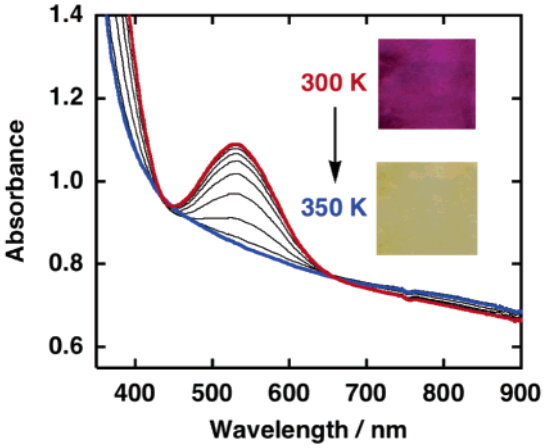

Figure 3. Electronic absorption spectra of (G0trz)Fe at different temperatures on heating from 300 (red curve) to 350 K (blue curve). Pictures were taken at 300 and 350 K.

Figure 4 shows that the χT values of (G0trz)Fe−(G2trz)Fe before the spin transition are not zero, although low-spin iron(II) species are diamagnetic. When the generation number (n) of the dendritic unit increased from 0 to 1 to 2, the χT value increased from 0.35 to 0.7 to 2.1 cm^3 K mol^{-1}, respectively. According to literatures,[15] χT values of coordination polymers of low-spin iron(II) species most likely originate from the chain-

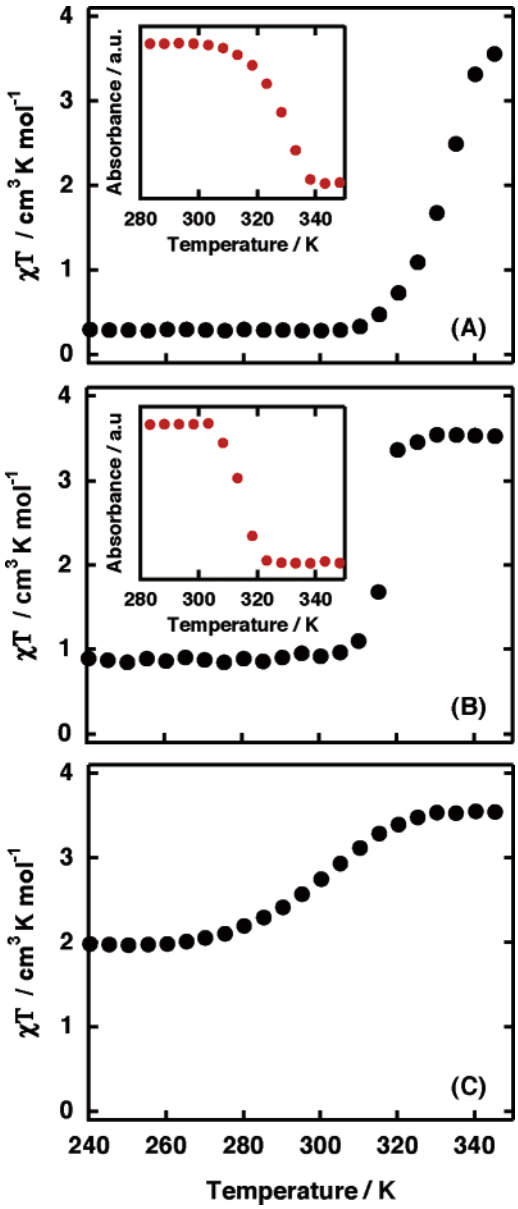

Figure 4. Magnetic susceptibilities of (G0trz)Fe (A), (G1trz)Fe (B), and (G2trz)Fe (C), upon heating. Inset: Changes in absorbance at 553 nm on heating (see Figure 3).

end iron(II) sites, which are hydrated and always adopt a high-spin state. Therefore, the χT values before the spin transition are informative of the number of the chain ends, which allows one to estimate the average degree of polymerization (D_p). Using the equation $D_p = 2\chi T_{350}/\chi T_{240}$, where χT_{240} and χT_{350} denote molar magnetic susceptibilities before (240 K) and after (350 K) the spin transition, respectively, the D_p values of (G0trz)Fe, (G1trz)Fe, and (G2trz)Fe were estimated as 20, 10, and 3, respectively. These values are in good agreement with those estimated from their elemental analysis data (Table 1) and are also consistent with the EXAFS profiles of (G0trz)Fe−(G2trz)-Fe, where the long-range $Fe^1-Fe^2-Fe^3$ scattering is obscure for the shortest-chain (G2trz)Fe. All of these observations

(15) (a) Kolnaar, J. J. A.; Dijk, G.; Kooijiman, H.; Spek, A. L.; Ksenofontov, V. G.; Gütlich, P.; Haasnoot, J. G.; Reedijk, J. *Inorg. Chem.* **1997**, *36*, 2433−2440. (b) Vos, G.; Febre, R. A.; Graff, R. A. G.; Haasnoot, J. G.; Reedijk, J. *J. Am. Chem. Soc.* **1983**, *105*, 1682−1683.

Table 1. Elemental Analysis Data of (G*n*trz)Fe ($n = 0-2$)

		Element				
(G*n*trz)Fe	D_p[a]	Fe	C	H	N	S
		Content in % (obsd/calcd)				
(G0trz)Fe	20	2.94/2.98	61.1/61.9	9.07/8.54	8.05/8.54	4.0/3.99
(G1trz)Fe	10	1.72/1.64	68.8/68.8	9.55/9.51	4.15/4.46	2.5/2.49
(G2trz)Fe	3	0.96/0.96	73.1/73.6	9.98/9.78	2.01/2.26	1.9/1.98

[a] D_p = average degree of polymerization.

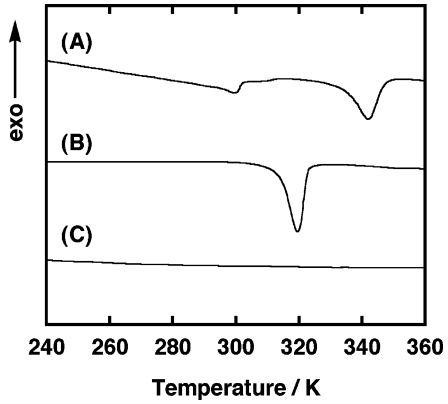

Figure 5. Differential scanning calorimetry (DSC) profiles of (G0trz)Fe (A), (G1trz)Fe (B), and (G2trz)Fe (C), upon heating at a rate of 5 K min^{-1}.

indicate that the supramolecular polymerization of dendritic triazole G*n*trz with iron(II) is impeded by larger dendrons.

Thermal Properties of (G*n*trz)Fe ($n = 0-2$). In the DSC profile, (G0trz)Fe exhibited an endothermic peak at 330−350 K (57−77 °C) upon heating (Figure 5A).[16] By reference to the temperature-dependent change in χT, this endothermic DSC peak is assigned to the spin transition. The ΔH and ΔS values of the endotherm were evaluated as 15.7 kJ mol^{-1} and 46.7 J mol^{-1} K^{-1}, respectively, which are typical of those reported for spin transition of iron(II) complexes.[17] Although one generation higher (G1trz)Fe displayed a similar DSC thermogram to that of (G0trz)Fe (Figure 5B), the endothermic peak characteristic of the spin transition was relatively sharp and observed at a lower temperature (312−322 K (39−49 °C)). Of further interest, the ΔH and ΔS values for this endothermic event of (G1trz)Fe were evaluated as 73.1 kJ mol^{-1} and 230.0 J mol^{-1} K^{-1}, respectively, which are much greater than those of ordinary spin transition, as observed for (G0trz)Fe. In sharp contrast, (G2trz)Fe with a low content of the iron(II) species hardly showed endothermic transitions under identical conditions (Figure 5C).

Structures of Self-Assembled (G*n*trz)Fe ($n = 0-2$). The abrupt spin-transition profile of (G1trz)Fe (Figure 4B), along with its extraordinary large ΔH and ΔS values (Figure 5B), suggests that the iron(II) sites in self-assembled (G1trz)Fe are strongly connected with one another and highly cooperate in the spin-transition event. In relation to this feature, (G1trz)Fe showed the most distinct X-ray diffraction (XRD) pattern among (G0trz)Fe−(G2trz)Fe (Figure 6).[18] It displayed an intense

(16) The thermogravimetric analysis (TGA) of the complexes showed no substantial weight loss upon heating to at least 150 °C. Therefore, these complexes are robust in the temperature range for spin transition below 100 °C.
(17) König, E. *Struct. Bonding* **1991**, *76*, 51−55.
(18) Percec et al.[5] have reported that a hexagonal phase formed from a core−shell rod with a high electron density in the core hardly shows (11) and (20) reflections in XRD. This may be the reason the (11) and (20) reflections are obscure in Figure 6.

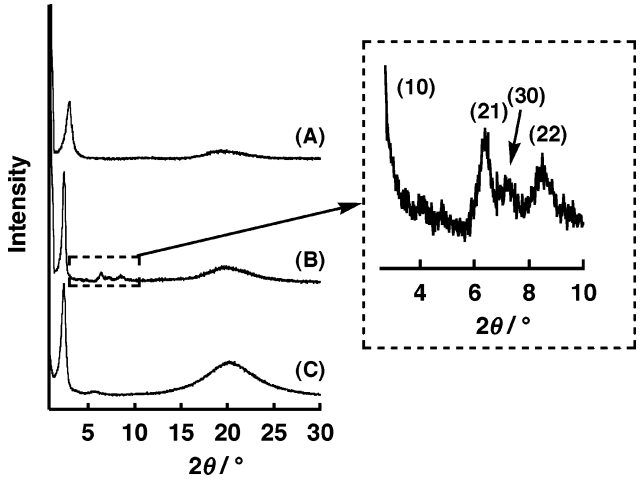

Figure 6. X-ray diffraction (XRD) profiles of (G0trz)Fe (A), (G1trz)Fe (B and inset), and (G2trz)Fe (C) at 296 K.

diffraction peak with a *d* spacing of 37.4 Å in the small-angle region and three minor peaks with *d* spacing values of 13.7, 12.1, and 10.4 Å (Figure 6B). These four peaks had a *d* spacing ratio close to $1:1/\sqrt{7}:1/\sqrt{9}:1/\sqrt{12}$ and were assigned to (10), (21), (30), and (22) diffractions of a 2D hexagonal column. From the *d* spacing value of the (10) diffraction, along with the Fe−Fe distance (3.7 Å, Figure 2B) as evaluated by EXAFS, the unit cell was calculated to be 43.2 Å in diameter and 3.7 Å in height ($V = 5.42$ nm^3, $W = 5.79 \times 10^{-21}$ g). Since the density of the material, measured using a gradient density column, was 1.07 g cm^{-3}, the unit cell was estimated to accommodate 2.8 units of G1trz. This number is very close to that requested from the stoichiometry of the 1:3 complexation between iron(II) and triazole. Thus, the dendritic wedges in self-assembled (G1trz)-Fe are densely packed around the oligomeric iron(II)−triazole backbone and perfectly fill the surrounding space (Scheme 1).

Likewise, (G0trz)Fe and (G2trz)Fe displayed an intense diffraction peak in the small-angle region (*d* spacing = 29.6 (Figure 6A) and 37.0 Å (Figure 6C)), but did not show other diffraction peaks. Nevertheless, if we assume that (G0trz)Fe and (G2trz)Fe also adopt a hexagonal columnar structure analogous to that of (G1trz)Fe, their unit cells are estimated to accommodate 4.1 and 1.6 units of G*n*trz, respectively. In contrast with the ideal case of (G1trz)Fe, where the unit cell is densely filled with the three G1trz units, G0trz is not large enough to fill the unit cell of (G0trz)Fe in an analogous manner, while the unit cell of (G2trz)Fe is not large enough to satisfy the requisite from the 1:3 complexation between iron(II) and G2trz. From these results, it is most likely that self-assembled (G0trz)Fe and (G2trz)Fe are structurally defective and frustrative, so that the iron(II) sites in these materials are hardly cooperative with one another for the spin transition.

Conclusions

We have demonstrated that poly(benzyl ether) dendrons bearing a triazole focal core (G*n*trz, $n = 0-2$) coordinate with iron(II) species to form the corresponding metal triazolate oligomers ((G*n*trz)Fe, $n = 0-2$) which can self-organize to give columnar assemblies with thermal spin-transition activity. The spin transition is accompanied by a slight volume change of the coordination sphere around the metal center, so that a domino effect can be expected when the iron(II) centers are strongly connected and cooperative with one another. The spin-transition profiles of self-assembled (G*n*trz)Fe ($n = 0-2$) were highly dependent on the generation number (*n*) of the dendritic unit. Among (G0trz)Fe−(G2trz)Fe, (G1trz)Fe was the best-behaved complex in terms of the abruptness of spin transition (cooperativity). The self-assembled structure of (G1trz)Fe is not frustrative, as the unit cell was densely filled with the three dendritic ligands, as required from the stoichiometry of the complexation. Cooperativity can enhance or amplify certain functions in self-organized states. The present study clearly indicates that dendrimers are useful components for functional soft materials in that they allow us to design "cooperativity".

Experimental Section

Materials and Synthesis. Tetrahydrofuran (THF) was refluxed over sodium and benzophenone ketyl under Ar and distilled just before use. 18-Crown-6 ether was recrystallized from acetonitrile, dried overnight under reduced pressure, and then stored under dry N_2. Triphenylphosphine was recrystallized from hexane before use. 4-Amino-1,2,4-triazole was recrystallized from THF and stored under N_2. K_2CO_3 was dried at 150 °C under reduced pressure before use. Other reagents were used as received.

Carboxylic acid-terminated poly(benzyl ether) dendrons, G*n*CO_2H ($n = 0-2$), were prepared in a manner similar to that previously reported.[19] Iron(II) methylsulfonate, $Fe(MeSO_3)_2 \cdot 3 \cdot 1H_2O$, was synthesized by mixing iron powder and methanesulfonic acid in water in the presence of ascorbic acid, followed by evaporation.

General Procedures for the Synthesis of G*n*trz ($n = 0-2$). To a THF solution of a mixture of G*n*CO_2H, triethylamine (1.3 equiv), and DBOP (1.3 equiv) stirred at room temperature for 30 min was added 4-amino-1,2,4-triazole (2.0 equiv). The mixture was refluxed for 30 min and cooled to room temperature and then filtered off from 4-amino-1,2,4-triazole which remained unreacted. The filtrate was evaporated to dryness under reduced pressure at room temperature, and the residue was chromatographed on silica with $CHCl_3$/MeOH (gradient from 100/0 to 97/3 in vol) as eluent, where the second fraction was collected and evaporated to dryness to leave G*n*trz as white solid in 90−96% yield.

G0trz: Yield 95%, after recrystallization from MeOH; ^{1}H NMR (500 MHz, $CDCl_3$) δ (ppm) 0.86 (6H, t, $J = 7.0$ Hz, CH_3), 1.24 (32H, m, $(CH_2)_8$), 1.40 (4H, m, $J = 7.0$ Hz, $OCH_2CH_2CH_2$), 1.76 (4H, m, $J = 7.0$ Hz, OCH_2CH_2), 3.92 (4H, t, $J = 7.0$ Hz, OCH_2), 6.66 (1H, t, $J = 2.0$ Hz, ArH), 7.17 (2H, d, $J = 2.0$ Hz, ArH), 8.20 (2H, s, triazole−H); ^{13}C NMR (125 MHz, $CDCl_3$) δ (ppm) 14.2, 22.6, 26.1, 29.2, 29.4, 29.5, 29.7, 32.0, 68.5, 106.0, 106.7, 131.8, 143.4, 160.5, 166.0; FT-IR (KBr; cm^{-1}) ν (NH) 3115, ν_{asym} (CH_2) 2920, ν_{sym} (CH_2) 2850, ν (C═O) 1670, ν (C═C) 1605, ν (N═C−N) 1552, ν (CONH) 1515, δ (CH_2) 1468, ν (C−O) 1169, δ (CH_2) 713, γ (trz) 631. MALDI-TOF-MS for $C_{33}H_{56}N_4O_3$: *m*/*z* calcd, 557.8 [M + H$^+$]; found, 557.6.

G1trz: Yield 96%, after reprecipitation from THF/MeOH; ^{1}H NMR (500 MHz, $CDCl_3$) δ (ppm) 0.85 (12H, t, $J = 7.0$ Hz, CH_3), 1.24 (64H, m, $(CH_2)_{12}$), 1.39 (8H, m, $J = 7.0$ Hz, $OCH_2CH_2CH_2$), 1.73 (8 H, m, $J = 7.0$ Hz, OCH_2CH_2), 3.90 (8H, t, $J = 7.0$ Hz, OCH_2), 4.96 (4H, s, benzyl CH_2), 6.34 (2H, t, $J = 2.0$ Hz, ArH), 6.48 (4H, d, $J = 2.0$ Hz, ArH), 6.79 (1H, t, $J = 2.0$ Hz, ArH), 7.27 (2H, d, $J = 2.0$ Hz, ArH), 8.19 (2H, s, triazole−H); ^{13}C NMR (125 MHz, $CDCl_3$) δ (ppm) 14.2, 22.7, 26.1, 29.3, 29.4, 29.5, 29.6, 29.7, 31.9, 68.1, 70.3, 100.8, 105.6, 106.6, 107.4, 132.0, 138.3, 143.3, 160.0, 160.3, 165.6; FT-IR (KBr; cm^{-1}) ν (NH) 3118, ν_{asym} (CH_2) 2921, ν_{sym} (CH_2) 2851, ν (C═O) 1684, ν (C═C) 1599, ν (N═C−N) 1540, ν (CONH) 1507, δ (CH_2) 1466, ν (C−O) 1166, δ (CH_2) 720, γ (trz) 619. MALDI-TOF-MS for $C_{71}H_{117}N_4O_3$: *m*/*z* calcd, 1138.70 [M + H$^+$]; found, 1137.1.

G2trz: Yield 90%; ^{1}H NMR (500 MHz, $CDCl_3$) δ (ppm) 0.85 (24H, t, $J = 7.0$ Hz, CH_3), 1.23 (128H, m, $(CH_2)_{12}$), 1.39 (16H, m, $J = 7.0$

(19) L'abbé, G.; Forier, B.; Dehaen, W. *Chem. Commun.* **1996**, 2143-2144.

Hz, $OCH_2CH_2CH_2$), 1.72 (16 H, m, $J = 7.0$ Hz, OCH_2CH_2), 3.88 (16H, t, $J = 7.0$ Hz, OCH_2), 4.90 (8H, s, benzyl CH_2), 4.97 (4H, s, benzyl CH_2), 6.36 (4H, t, $J = 2.0$ Hz, ArH), 6.50 (8H, d, $J = 2.0$ Hz, ArH), 6.53 (2H, t, $J = 2.0$ Hz, ArH), 6.61 (4H, d, $J = 2.0$ Hz, ArH), 6.78 (1H, t, $J = 2.0$ Hz, ArH), 7.10 (2H, d, $J = 2.0$ Hz, ArH), 8.21 (2H, s, triazole−H); ^{13}C NMR (125 MHz, $CDCl_3$) δ (ppm) 14.2, 22.7, 26.1, 29.3, 29.4, 29.5, 29.6, 29.7, 30.9, 31.9, 68.1, 70.2, 100.7, 100.9, 105.7, 106.2, 107.4, 138.3, 138.7, 143.1, 160.0, 160.3; FT-IR (KBr; cm^{-1}) ν (NH) 3126, ν_{asym} (CH_2) 2923, ν_{sym} (CH_2) 2853, ν (C═O) 1692, ν (C═C) 1597, δ (CH_2) 1454, ν (C−O) 1165, δ (CH_2) 721, γ (trz) 618. MALDI-TOF-MS for $C_{147}H_{237}N_4O_3$: *m*/*z* calcd, 2300.46 [M + H^+]; found, 2300.00.

General Procedures for the Synthesis of (G*n*trz)Fe (*n* = 1−3). To a MeOH/THF (5:1 in vol) solution of G*n*trz was added at 60 °C a MeOH/THF (5:1 in vol) solution of $Fe(MeSO_3)_2 \cdot 3 \cdot 1H_2O$ (5 equiv) containing a small amount of ascorbic acid, and the reaction mixture was stirred for 5 min and cooled to room temperature. A purple precipitate thus formed was collected by filtration, washed with MeOH, and dried under reduced pressure at room temperature to leave (G*n*trz)-Fe as a purple solid quantitatively.

(G0trz)Fe: FT-IR (KBr; cm^{-1}) ν (OH) 3446, ν (NH) 3100, ν_{asym} (CH_2) 2923, ν_{sym} (CH_2) 2853, ν (C═O) 1696, ν (C═C) 1604, ν (N═C−N) 1561, ν (CONH) 1519, δ (CH_2) 1465, ν (C−O) 1167, ν_{asym} (O═S═O) 1206, ν_{sym} (O═S═O) 1046, δ_{asym} (O═S═O) 776, δ (CH_2) 721, γ (trz) 622, δ_{sym} (O═S═O) 554.

(G1trz)Fe: FT-IR (KBr; cm^{-1}) ν (OH) 3446, ν (NH) 3091, ν_{asym} (CH_2) 2923, ν_{sym} (CH_2) 2853, ν (C═O) 1695, ν (C═C) 1598, ν (N═C−N) 1563, ν (CONH) 1520, δ (CH_2) 1464, ν (C−O) 1166, ν_{asym} (O═S═O) 1210, ν_{sym} (O═S═O) 1045, δ_{asym} (O═S═O) 776, δ (CH_2) 721, γ (trz) 625, δ_{sym} (O═S═O) 553.

(G2trz)Fe: FT-IR (KBr; cm^{-1}) ν (OH) 3446, ν (NH) 3093, ν_{asym} (CH_2) 2923, ν_{sym} (CH_2) 2853, ν (C═O) 1696, ν (C═C) 1597, δ (CH_2) 1463, ν (C−O) 1165, ν_{asym} (O═S═O) 1209, ν_{sym} (O═S═O) 1045, δ_{asym} (O═S═O) 778, δ (CH_2) 721, γ (trz) 621, δ_{sym} (O═S═O) 553.

Measurements. ^{1}H and ^{13}C NMR spectra were recorded in $CDCl_3$ at 25 °C on a JEOL model NMR-EXCALIBUR, operating at 500 and 125 MHz, respectively. MALDI-TOF-MS spectra were recorded on an Applied Biosystems model BioSpectrometry Workstation Voyager-DE STR in a reflector mode using dithranol as a matrix. Infrared spectra were recorded on a JASCO model FTIR-660 plus in a range of 400−4000 cm^{-1} at room temperature with KBr disks. Variable-temperature IR spectra were recorded on a JEOL model JIR-6000 FTIR at 20−100 °C. DSC measurements were performed on a Mettler model DSC 822e. Temperature and enthalpy were calibrated with standard indium (430 K, 3.3 J mol^{-1}) and Zn (692.7 K, 12 J mol^{-1}) samples using sealed sample pans. Heating profiles were recorded and analyzed with a Mettler model STARe system. Magnetic susceptibility measurements were performed on a Quantum Design model DSM-8 susceptometer equipped with a Quantum Design model MPMS-5S SQUID magnetometer, operating at 240−350 K. Magnetic data were corrected for magnetization of the sample holder and diamagnetic contributions, which were evaluated from the Pascal constants. Fe K-edge EXAFS spectra were taken in the transmission mode at Beamline 15C of the Photon Factory. Spectra were recorded for a homogeneous pallet sample embedded between two X-ray-transparent polymer films in a range of 6910−8110 eV. The REX2000 (Rigaku) program was used for data processing. X-ray diffraction (XRD) patterns were recorded at room temperature on a Rigaku model RINT-2500 counter diffractometer with a Cu Kα radiation source. Density measurements were carried out using a gradient density column (water/ethylene glycol) with glass beads as standards.

Acknowledgment. We thank Kyocera Chemical for providing DBOP. We thank Dr. K. Okitsu of the High Power X-ray Laboratory (University of Tokyo) for EXAFS measurement under the approval of Photon Factory Program Advisory Committee (No. 2003G203). T.F. thanks JSPS Research Fellowships for Young Scientists.

JA050275K